Low Temperature Activation of Carbon Dioxide by Ammonia in Methane Dry Reforming—A Thermodynamic Study

Anand Kumar

Department of Chemical Engineering, Qatar University, P. O. Box 2713, Doha, Qatar; akumar@qu.edu.qa
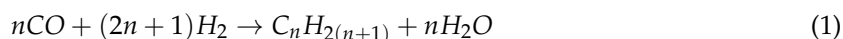
Abstract: Methane dry reforming (MDR) is an attractive alternative to methane steam reforming for hydrogen production with low harmful environmental emissions on account of utilizing carbon dioxide in the feed. However, carbon formation in the product stream has been the most challenging aspect of MDR, as it leads to catalyst deactivation by coking, prevalent in hydrocarbon reforming reactions. Common strategies to limit coking have mainly targeted catalyst modifications, such as by doping with rare earth metals, supporting on refractory oxides, adding oxygen/steam in the feed, or operating at reaction conditions (e.g., higher temperature), where carbon formation is thermodynamically restrained. These methods do help in suppressing carbon formation; nonetheless, to a large extent, catalyst activity and product selectivity are also adversely affected. In this study, the effect of ammonia addition in MDR feed on carbon suppression is presented. Based on a thermodynamic equilibrium analysis, the most significant observation of ammonia addition is towards low temperature carbon dioxide activation to methane, along with carbon removal. Results indicate that ammonia not only helps in removing carbon formation, but also greatly enriches hydrogen production.

Keywords: methane dry reforming; carbon dioxide conversion; ammonia-assisted reforming; thermodynamic equilibrium analysis

1. Introduction

The reaction $CH_4 + CO_2 \rightarrow CO + H_2$ or methane dry reforming (MDR) for producing hydrogen from methane provides an alternative way to the industrially used methane steam reforming (MSR) [1–5]. The advantage of MDR reaction is that it uses CO_2 as a feed, thus ameliorating the environmental impact by decreasing the concentration of this ubiquitous greenhouse gas, and generating a ratio of H_2 and CO that can be adjusted to obtain the required synthesis gas (syngas) composition. Starting from syngas, using Fischer–Tropsch chemistry, long chain hydrocarbons and liquid fuels can be produced on transition metal oxide catalysts, as described in Equation (1):

$$nCO + (2n+1)H_2 \rightarrow C_nH_{2(n+1)} + nH_2O \tag{1}$$

The main disadvantage of the MDR reaction is that the catalysts used in this reaction undergo severe deactivation, primarily due to carbon formation, also known as coking, limiting the lifetime of the catalysts [3,6–11]. Supported noble metals suffer less deactivation, but are costly, and the use of alkali promoters increases time on stream (TOS), but decreases activity and selectivity [3,9,12–15]. Mechanistic studies indicate the dissociation of methane on metal surfaces proceeds via two widely accepted reaction pathways: Firstly, by direct dissociation, and secondly, by indirect dissociation of intermediate species [7,10,16,17]. The direct dissociation is anticipated to take place at a high

temperature, while the low temperature conditions are expected to favor indirect dissociation through reaction intermediates (e.g., CH_x or formyl group) [18], where the oxygen is supplied from CO_2 or via the support [19]. Some reports indicate the activation of methane to be favored on metal active sites, while that of carbon dioxide on the support during MDR [20]. Other reports indicate that supports do play a role in methane activation and the acidity or basicity of the support can influence the activation of methane [20,21] and, in some cases, the activation of CH_4 is reported to require the availability of adsorbed oxygen, usually coming from the supports [22]. Methane reforming in the availability of CO_2 or other oxidants (steam, oxygen, or air) indicates low carbon formation and high syngas yield [23–26] with a varying ratio of H_2/CO based on the nature of support used.

Recent literature [19,27–29] has summarized the status of coke formation in various hydrocarbon reforming catalysts susceptible to coke poisoning. Mechanistic studies conducted on different catalyst surfaces suggest the following intermediate reactions to be the main contributors in coke formation in MDR and other hydrocarbon reforming reactions [19]:

- The Boudouard reaction:

$$2CO \rightarrow CO_2 + C \tag{2}$$

- Reverse carbon gasification:

$$CO + H_2 \rightarrow H_2O + C \tag{3}$$

- Dehydrogenation of hydrocarbons:

$$C_mH_n \rightarrow n/2H_2 + mC \tag{4}$$

- Polymerization of ethylene to coke:

$$C_2H_4 \rightarrow coke \tag{5}$$

- Conversion of acetone to mesityl oxide $((CH_3)_2C = CHCOCH_3)$, which can further oligomerize to generate coke [30].

The Boudouard reaction is understood to be the main cause of carbon formation at a low temperature, whereas dehydrogenation of intermediate hydrocarbons at a high temperature favors coke formation [3,19]. These intermediate reactions are observed in both hydrocarbon and oxygenated hydrocarbon reforming, indicating similar catalysts could work in both cases for suppressing coke formation.

Although various studies have been conducted on the design of effective catalysts for MDR reactions and a considerable progress has been made in the direction of understanding the mechanism of deactivation, nonetheless, carbon formation still remains a great challenge that limits the MDR catalysts' life cycle. Thermodynamic studies indicate a significant decrease in carbon formation in reforming oxygenated compounds when certain chemical additives are introduced in the feed [31,32], where carbon suppression is also accompanied by hydrogen enrichment [31,32]. In this work, the effect of ammonia addition in the MDR feed stream on coke formation is investigated. This study is based on the thermodynamic equilibrium analysis to obtain product distribution between 300–1000 K. My research group is primarily working on the catalysts' synthesis using combustion-based techniques for hydrocarbon reforming reactions [33–48]. While the experimental work on catalyst development for MDR is still underway, the results on thermodynamic equilibrium analysis are presented here to understand the favorable reaction conditions. Considering the ongoing work on ammonia to be used as a hydrogen storage chemical [49,50], this study becomes more relevant and also investigates the total hydrogen enrichment and quality of syngas produced in ammonia-assisted MDR. Unlike methane partial oxidation, hydrogen amount is not expected to be compromised while removing the deposited carbon here. The thermodynamic calculation methodology applied in this study is briefly presented in the following section.
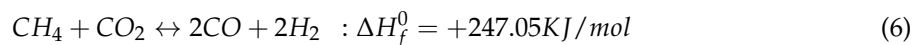
2. Thermodynamic Calculations

The conditions of equilibrium product distribution at a given temperature pressure were calculated using a software package "THERMO". The program works on the basis of minimization of Gibbs free energy in a multiphase and multicomponent system, assuming the condensed phases to be immiscible and the gases to follow ideal gas law. The details of the program can be found in the reference manual and other publications [31,32,51]. Table 1 contains the enthalpy of formation of various compounds that are used in thermodynamic analysis. It should be noted that the "THERMO" program has a comprehensive database containing products with other possible atomic combinations of C, H, N, and O, and does not limit the optimization to only to the components listed in Table 1.

Table 1. The standard enthalpy of formation for various compounds used in this study [52].

Compound	Enthalpy of Formation (ΔH_f^0), KJ/mol
CH_4	−74.6
CO_2	−393.51
H_2O (g)	−241.826
NH_3	−45.94
CO	−110.53
H_2	0
N_2	0
C (graphite)	0

3. Results and Discussion

Thermodynamic equilibrium product distribution for methane dry reforming using 1:1 molar ratio of $CH_4:CO_2$ (Equation (5)) at 1 atm. pressure and a temperature range of 300–1000 K is shown in Figure 1a.

$$CH_4 + CO_2 \leftrightarrow 2CO + 2H_2 \quad : \Delta H_f^0 = +247.05 KJ/mol \tag{6}$$

Looking at the distribution of various compounds (Figure 1a), it is clear that elemental carbon and water are the two most stable products at low temperature and both start to decrease as temperature increases. Methane concentration, however, increases to a maximum value of 0.39 moles at 600 K before starting to decrease and gradually reaching ~100% conversion at 1000 K. Carbon dioxide shows a similar trend, with an increasing value at lower temperature reaching to a maximum of ~0.55 moles at 800 K before starting to decrease. There is no CO formation until 600 K, whereas hydrogen starts to appear as early as 400 K itself and both CO and H_2 show an exponential increase in concentration with temperature, indicating that higher temperature is more favorable for syngas formation and low temperatures are suitable for coking. Similar trends were obtained by Pakhare et al. [3,53] while investigating the effect of temperature on carbon formation in dry reforming of methane, indicating that only temperatures above 900 °C (1173 K) are suitable for carbon-free products.
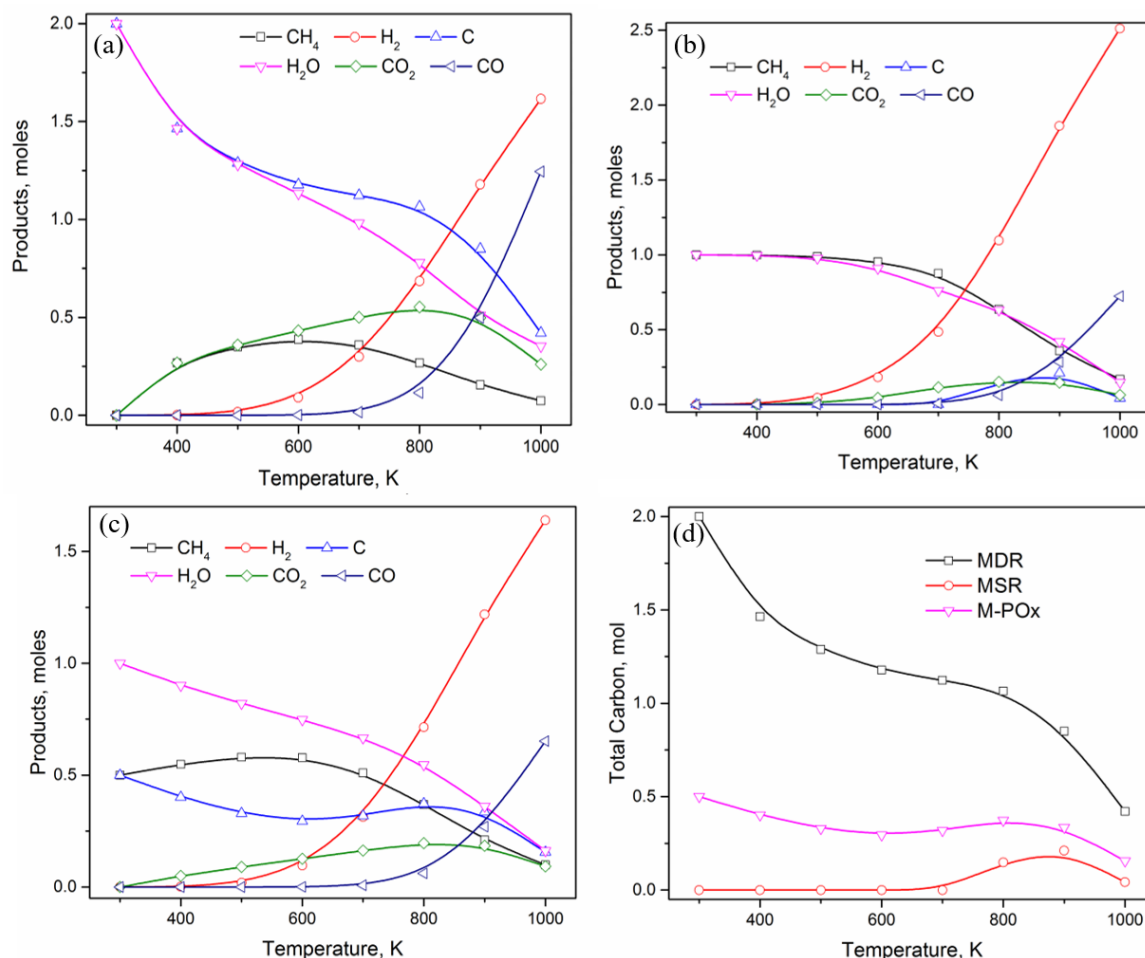
Figure 1. Product distribution in (**a**) methane dry reforming, (**b**) methane steam reforming, (**c**) methane partial oxidation, (**d**) total carbon formation in all the three reactions. All the calculations were performed at 1 atm pressure.

Extending the thermodynamic investigations to other commonly used methane-reforming reactions, that is, methane steam reforming (MSR: $CH_4 + H_2O$, Figure 1b) and methane partial oxidation (M-POx: $CH_4 + \frac{1}{2}O_2$, Figure 1c), a decrease in carbon formation is very clear in the presence of steam and oxygen, respectively. However, a careful observation indicates that methane conversion is also inferior in these two reactions at low temperature values. Starting with the same initial methane amount of 1 mole, comparing the equilibrium amount of methane present in the three systems at 800 K, the lowest conversion is observed in MSR with 0.64 moles of unreacted methane, followed by M-POx with 0.37 moles and MDR with only 0.27 moles. Nonetheless, conversion of methane directly relates to the amount of carbon formed at lower temperature values, as the other product containing carbon (i.e., CO) is insignificant for temperatures below 800 K. Figure 1d combines the trend of carbon formation in the three reactions, showing profiles with maximum carbon generation in MDR, followed by MSR and M-POx respectively. The effect of temperature on carbon content is clearly indicated by exposing two regions of distinct carbon growth patterns. For T < 700 K, carbon content monotonically decreases in MDR and M-POx, whereas no carbon was observed in MSR. A deflection in carbon profile is observed in MDR and M-POx between 700 K–1000 K, while in MSR, carbon starts to appear at 700 K, reaches a maximum value of 0.21 moles at 900 K before decreasing to 0.04 moles at 1000 K. Throughout the investigated temperature range of 300–1000 K, MDR shows the highest carbon formation, though gradually decreasing with temperature, forming an ideal system for our investigation of ammonia-assisted methane dry reforming and observing the effect of ammonia on the reduction of carbon.

Currently, a number of research activities are targeting ammonia synthesis as a means of hydrogen storage [49,50,54]. Ammonia is a clean source for on-demand hydrogen generation, providing high hydrogen density and no harmful environmental emissions, as nitrogen is the only byproduct [49,50,54]. The addition of ammonia alongside carbon dioxide in MDR could help in alleviating coke formation and increasing the catalyst life cycle, along with increasing the total hydrogen production. The thermodynamic feasibility tests are being performed at this stage and the experimental validations are to follow up in future communications.

Figure 2 shows the effect of ammonia (1 mol) addition on the product distribution in MDR systems. Ammonia is anticipated to decompose, producing nitrogen and hydrogen gases, as displayed by a constant amount of 0.5 moles of nitrogen throughout the temperature range of investigation and an increase in hydrogen amount as compared to MDR without ammonia. It should be noted that ammonia is completely utilized and practically no amount is present starting from 300 K until 1000 K (Figure 2a). Other products' distribution indicates a considerable increase in CH_4 moles and a slight increase in H_2O and CO moles, whereas a decrease in carbon and CO_2 moles is observed. This trend is clearly illustrated by comparing the product distribution at 800 K, as shown in Figure 2b. A significant increase in CH_4, H_2, and H_2O is seen as compared to a decrease in C and CO_2, whereas the amount of CO is only slightly affected. An increase in CH_4 moles and a simultaneous decrease in CO_2 moles indicates an improved CO_2 activation by ammonia towards CH_4, C, and CO formation.
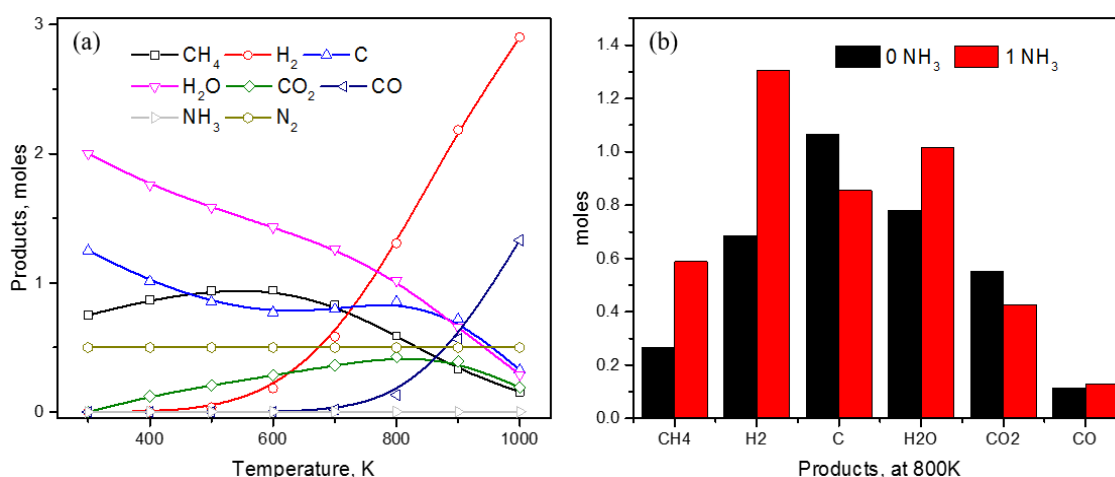

Figure 2. (**a**) Product distribution in ammonia-assisted methane dry reforming ($CH_4 + CO_2 + NH_3$); (**b**) comparison in product amount at 800 K with and without NH_3 addition.

The addition of one mole of ammonia in an MDR system has certainly helped in reducing the carbon content, but only to a limited extent. In order to eliminate carbon completely, an extra amount of ammonia is required, as presented in Figure 3. For a low temperature range of 300–800 K, carbon can be completely removed by increasing the ammonia content to 4 moles for each mole of methane used. Carbon content at 300 K gradually decreases from a value of 2 moles in the absence of ammonia to values of 1.25, 0.5, and 0 moles as the ammonia moles are increased to 1, 2, and 4, respectively. Thus, 4 moles of ammonia is sufficient for a carbon-free product in methane dry reforming at low temperature values, but it is not enough for high temperature operations with T > 800 K, where carbon formation peaks at T ~900 K before decreasing (as shown in Figure 3a). Comparing the carbon content in MDR products at 900 K (Figure 3b), additional ammonia up to 6 moles will be required for complete removal of carbon.
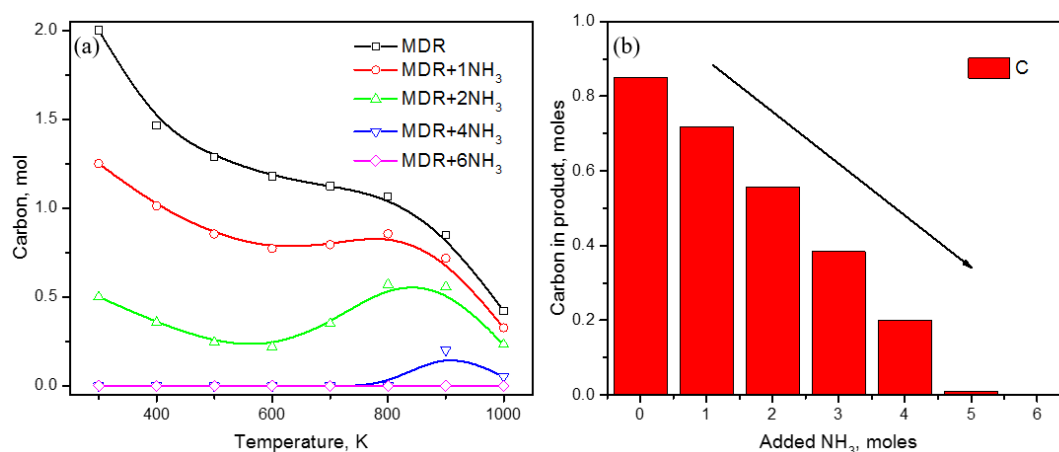
Figure 3. Effect of ammonia content on carbon formation in methane dry reforming; (**a**) at temperature 300–1000 K, (**b**) at temperature = 900 K.

As the inclusion of ammonia in MDR eliminates carbon formation, questions arise about the nature of products this carbon gets converted to. As shown earlier in Figure 2b, among the carbon-containing compounds, only methane and carbon monoxide show an increase in amount upon ammonia addition. This observation indicates that ammonia lowers the overall conversion of methane to carbon, whereas it facilitates carbon dioxide conversion as some amount of carbon dioxide is transformed into carbon monoxide (Figure 2b). This effect was further studied in detail, keeping in mind that approximately 6 moles of ammonia is required for carbon-free product distribution throughout the temperature range of 300–1000 K that is expected to create a strong reducing environment. Looking at the trends in Figure 4a, addition of high concentration of ammonia not only decreases the reactivity of methane, but also promotes methane formation at low temperature ranges until 700 K (Figure 4a). The methane amount increases from zero moles at 300 K in MDR to 0.75, 1.5, and 2 moles upon addition of 1, 2, and 4 moles of ammonia (Figure 4b); afterwards, the CH_4 value remains constant due to the lack of a carbon source, as only 2 moles of CH_4 can be produced in the MDR system ($CH_4 + CO_2$). Therefore, thermodynamically, it is very clear that ammonia can completely convert carbon dioxide to methane at lower temperature, which follows until 600 K as no decline in the methane amount is observed for T < 600 K. Increasing temperature beyond 600 K shows methane being actively converted to some other products, as indicated by the sharp downward trends in Figure 4a, with minimum values at 1000 K. Even at higher temperatures (1000 K), the addition of ammonia increases the methane amount in products with values of 0.15, 0.24, 0.32, 0.4, 0.47, and 0.5 for increasing NH_3 values from 1–6 moles (Figure 4b), as compared to approx. 0.1 moles of methane in the absence of NH_3.
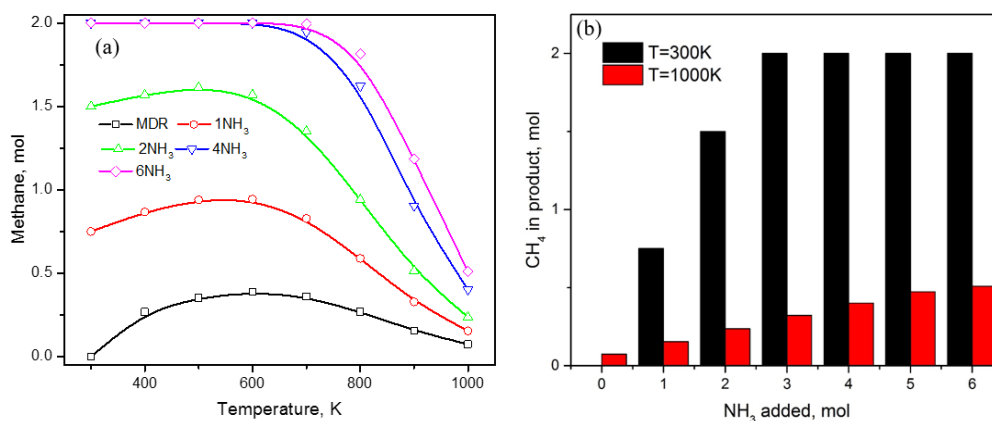

Figure 4. (**a**) Effect of ammonia content in MDR on methane; (**b**) comparison in methane amount in presence of NH_3 at 300 K and 1000 K with regard to no NH_3 in DMR.

Applying the principle of conservation of elements, an increase in the methane amount at low temperature could only result from a decrease in the carbon dioxide amount. As indicated in Figure 5a, the amount of CO_2 consistently decreases by increasing the ammonia content, while with CO being absent in the product until 600 K and the amount of carbon consistently decreasing, the selectivity for direct methane formation from CO_2 increases rapidly in the presence of NH_3. No CO_2 is observed for $NH_3 \geq 4$ moles until 600 K and only at higher temperature, whereas some CO_2 is observed with maximum value at T ≈ 800–900 K. Keeping track of CO_2 moles at 900 K, only 0.19 moles are left for $NH_3 = 6$ moles that also decreases further at 1000 K.
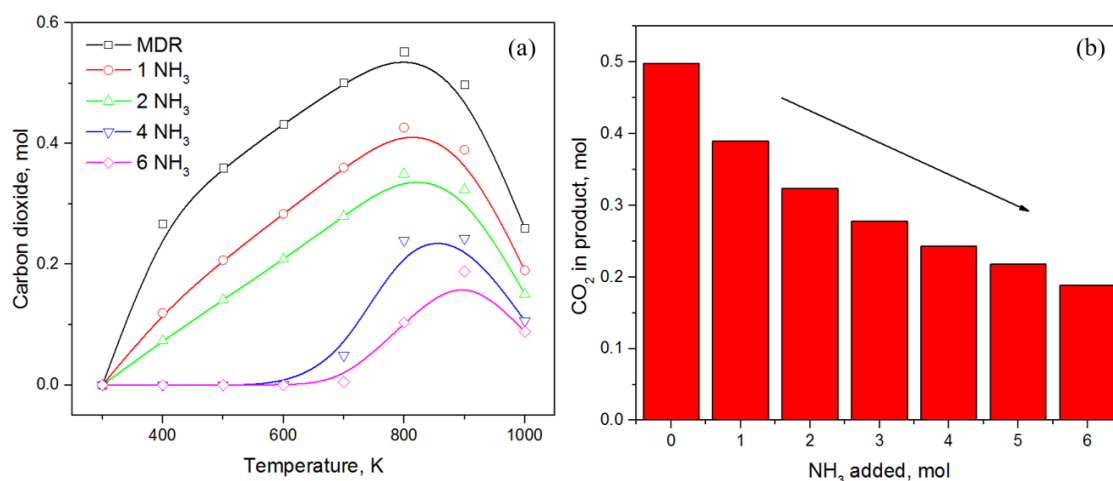

Figure 5. (**a**) Effect of ammonia content in DMR on CO_2 in product; (**b**) a decreasing trend in CO_2 amount in presence of NH_3 at 900 K.

Looking at the other carbon-containing product—CO in Figure 1b, Figure 2a, and Figure 6a—it is clear that CO is not generated until 600 K even if large amounts of NH_3 is added to the MDR system. The generation of CO happens only at T > 600 K and grows exponentially thereafter. Addition of NH_3 only has a slight effect, which is not as significant compared to other carbon-containing products like CO_2, CH_4, and C. Nonetheless, the overall impact of ammonia is a slight improvement in CO content, most significantly at T = 1000 K (Figure 6b), where CO moles vary from 1.2 moles to 1.4 moles. Hydrogen, on the other hand, is expected to experience the biggest increase in quantity due to ammonia being an additional source along with methane (Figure 7). For MDR and low amounts of NH_3 (≤2 mol), hydrogen generation starts only after T ≥ 600 K, a trend similar to CO production, before growing rapidly (Figure 7a). Low temperature conditions favor water production (Figure 1a, Figure 2a, and Figure 7b), which decreases gradually with an increase in temperature while increasing the hydrogen content in the product. As ammonia concentration is increased, water is preferentially produced and reaches the maximum value of 2 moles, limited by the number of oxygen atoms in the system coming from CO_2, before the excess hydrogen atoms are distributed among other products, such as CH_4 and H_2 (Figures 4a and 7). Looking at the trends of CH_4, CO_2, H_2, and H_2O in the presence of excess amount of NH_3 (≥4 mol), it appears as if carbon dioxide is transformed into methane at low temperature values (T < 600K), which undergoes steam reforming to produce syngas that is a combination of hydrogen and carbon monoxide. Therefore, it can easily be said that syngas production in the presence of ammonia is a result of MSR at high temperature, where ammonia facilitates excess methane and water generation at low temperature to be further utilized in MSR at high temperature.
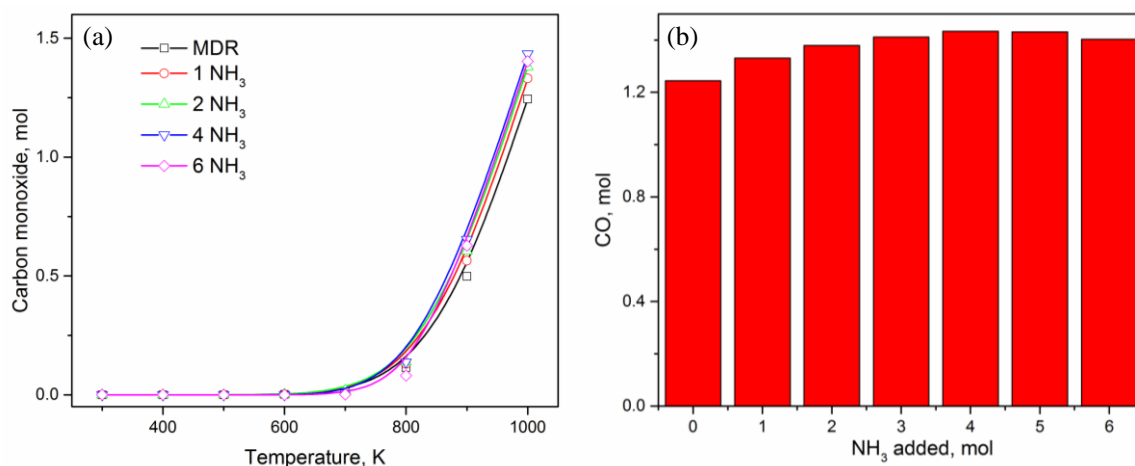
Figure 6. (**a**) Effect of ammonia content in DMR on CO in product; (**b**) CO amount in presence of NH_3 at 1000 K.
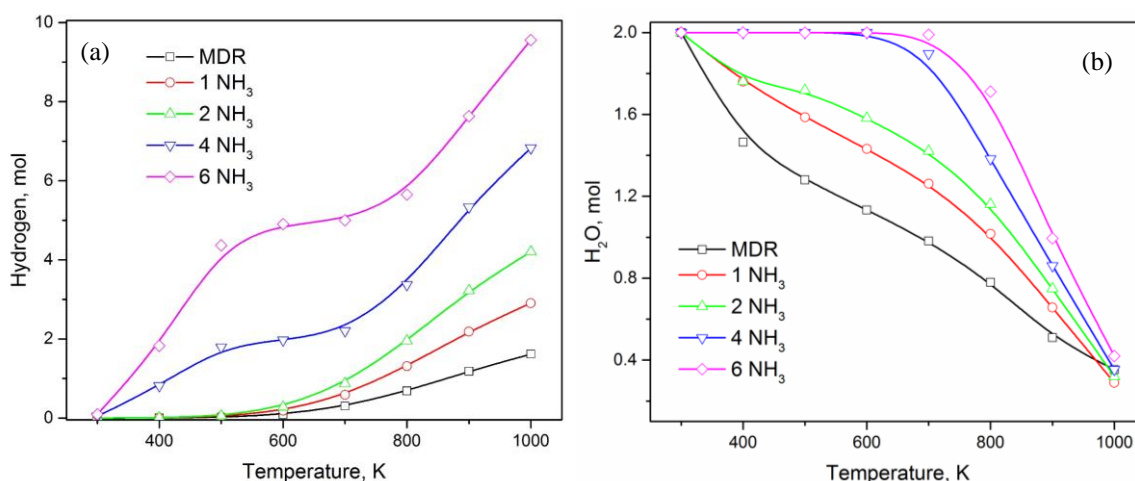

Figure 7. (**a**) Effect of ammonia content in DMR on H_2 in product, and (**b**) H_2O in product.

Figure 8 summarizes the results obtained so far while showing the carbon content in the product with syngas quality (H_2/CO ratio, Figure 8a) and simultaneously comparing the influence of ammonia in all carbon-containing products at 1000 K (Figure 8b). The addition of ammonia removes carbon from product, while it increases hydrogen production. On the other hand, the addition of ammonia does not affect CO production as much, and favors methane formation. As a result, carbon atom is distributed among CO_2, CH_4, and C as the ammonia amount is changed while maintaining a constant level of CO in the product. Thus, in the absence of further CO generation, the H_2/CO ratio appears to increase linearly with ammonia (Figure 8a).
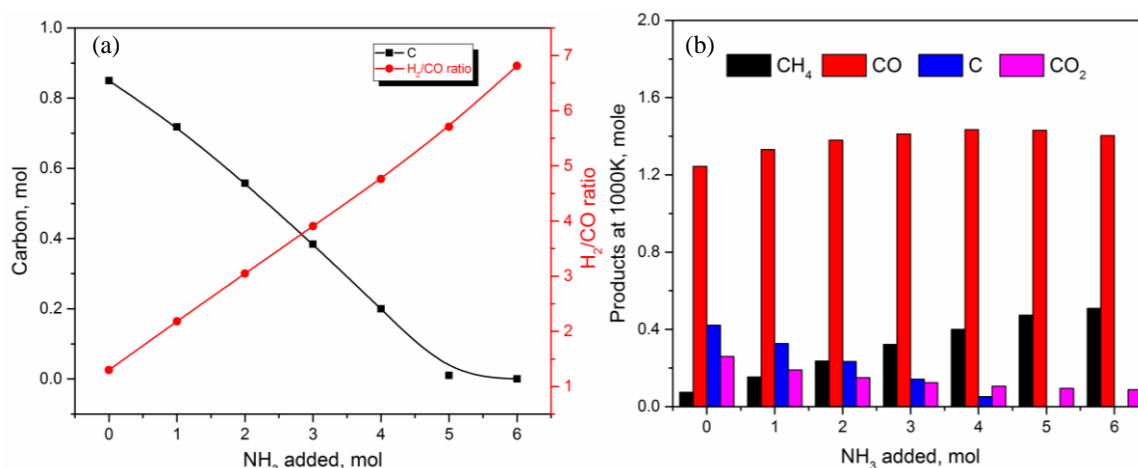
Figure 8. (**a**) Effect of ammonia content on syngas quality (H_2/CO ratio) and carbon content at 1000 K; (**b**) distribution of carbon-containing products at 1000 K as a function of ammonia content.

4. Conclusions

Carbon formation is a severe challenge in methane-reforming reactions, particularly MDR (methane dry reforming). Based on the thermodynamic calculations for equilibrium product distribution, it is clear that the carbon content in product can be minimized while simultaneously enhancing hydrogen generation by utilizing ammonia as a reducing agent in the MDR feed. Based on detailed product analysis with temperature, it is concluded that ammonia favors water and methane production at low temperature (T < 600 K), which, through the mechanism of methane steam reforming, produces hydrogen and carbon monoxide at elevated temperature values (T > 600 K). The addition of ammonia somehow does not significantly affect CO, as most of the carbon gets distributed among CO_2, C, and CH_4. A complete carbon-free product distribution is possible by using $NH_3 \geq 4$ moles for each mole of methane, resulting in an H_2/CO ratio above 5.5 mol/mol. The most significant role of ammonia is towards CO_2 conversion to methane at low temperature, in addition to producing high quantity of hydrogen.

Conflicts of Interest: The authors declare no conflict of interest. The founding sponsors had no role in the design of the study; in the collection, analyses, or interpretation of data; in the writing of the manuscript, and in the decision to publish the results.

References

1. Wang, S.; Lu, G.; Millar, G.J. Carbon dioxide reforming of methane to produce synthesis gas over metal-supported catalysts: State of the art. *Energy Fuels* **1996**, *10*, 896–904. [CrossRef]
2. Brungs, A.J.; York, A.P.; Claridge, J.B.; Márquez-Alvarez, C.; Green, M.L. Dry reforming of methane to synthesis gas over supported molybdenum carbide catalysts. *Catal. Lett.* **2000**, *70*, 117–122. [CrossRef]
3. Pakhare, D.; Spivey, J. A review of dry (CO_2) reforming of methane over noble metal catalysts. *Chem. Soc. Rev.* **2014**, *43*, 7813–7837. [CrossRef] [PubMed]
4. Dębek, R.; Motak, M.; Grzybek, T.; Galvez, M.E.; da Costa, P. A short review on the catalytic activity of hydrotalcite-derived materials for dry reforming of methane. *Catalysts* **2017**, *7*, 32. [CrossRef]
5. Seo, H.O. Recent Scientific Progress on Developing Supported Ni Catalysts for Dry (CO_2) Reforming of Methane. *Catalysts* **2018**, *8*, 110. [CrossRef]

6.　Messaoudi, H.; Thomas, S.; Djaidja, A.; Slyemi, S.; Barama, A. Study of La_xNiO_y and La_xNiO_y/$MgAl_2O_4$ catalysts in dry reforming of methane. *J. CO_2 Util.* **2018**, *24*, 40–49. [CrossRef]

7.　Budiman, A.W.; Song, S.; Chang, T.; Shin, C.; Choi, M. Dry reforming of methane over cobalt catalysts: A literature review of catalyst development. *Catal. Surv. Asia* **2012**, *16*, 183–197. [CrossRef]

8.　Liu, W.; Li, L.; Zhang, X.; Wang, Z.; Wang, X.; Peng, H. Design of Ni-ZrO_2@SiO_2 catalyst with ultra-high sintering and coking resistance for dry reforming of methane to prepare syngas. *J. CO_2 Util.* **2018**, *27*, 297–307. [CrossRef]

9.　Li, S.; Gong, J. Strategies for improving the performance and stability of Ni-based catalysts for reforming reactions. *Chem. Soc. Rev.* **2014**, *43*, 7245–7256. [CrossRef] [PubMed]

10.　Shah, Y.T.; Gardner, T.H. Dry Reforming of Hydrocarbon Feedstocks. *Catal. Rev.* **2014**, *56*, 476–536. [CrossRef]

11.　Park, J.; Yeo, S.; Chang, T. Effect of supports on the performance of Co-based catalysts in methane dry reforming. *J. CO_2 Util.* **2018**, *26*, 465–475. [CrossRef]

12.　Djaidja, A.; Libs, S.; Kiennemann, A.; Barama, A. Characterization and activity in dry reforming of methane on NiMg/Al and Ni/MgO catalysts. *Catal. Today* **2006**, *113*, 194–200. [CrossRef]

13.　Albarazi, A.; Beaunier, P.; da Costa, P. Hydrogen and syngas production by methane dry reforming on SBA-15 supported nickel catalysts: On the effect of promotion by $Ce_{0.75}Zr_{0.25}$ O_2 mixed oxide. *Int. J. Hydrog. Energy* **2013**, *38*, 127–139. [CrossRef]

14.　Tsyganok, A.I.; Inaba, M.; Tsunoda, T.; Uchida, K.; Suzuki, K.; Takehira, K.; Hayakawa, T. Rational design of Mg–Al mixed oxide-supported bimetallic catalysts for dry reforming of methane. *Appl. Catal. A General* **2005**, *292*, 328–343. [CrossRef]

15.　Sokolov, S.; Kondratenko, E.V.; Pohl, M.; Barkschat, A.; Rodemerck, U. Stable low-temperature dry reforming of methane over mesoporous La_2O_3-ZrO_2 supported Ni catalyst. *Appl. Catal. B: Environ.* **2012**, *113*, 19–30. [CrossRef]

16.　Delgado, K.H.; Maier, L.; Tischer, S.; Zellner, A.; Stotz, H.; Deutschmann, O. Surface reaction kinetics of steam-and CO_2-reforming as well as oxidation of methane over nickel-based catalysts. *Catalysts* **2015**, *5*, 871–904. [CrossRef]

17.　Ha, Q.L.M.; Armbruster, U.; Atia, H.; Schneider, M.; Lund, H.; Agostini, G.; Radnik, J.; Vuong, H.T.; Martin, A. Development of active and stable low nickel content catalysts for dry reforming of methane. *Catalysts* **2017**, *7*, 157. [CrossRef]

18.　Bradford, M.; Vannice, M. CO_2 reforming of CH_4. *Catal. Rev.* **1999**, *41*, 1–42. [CrossRef]

19.　Mattos, L.V.; Jacobs, G.; Davis, B.H.; Noronha, F.B. Production of hydrogen from ethanol: Review of reaction mechanism and catalyst deactivation. *Chem. Rev.* **2012**, *112*, 4094–4123. [CrossRef] [PubMed]

20.　Bitter, J.; Seshan, K.; Lercher, J. On the contribution of X-ray absorption spectroscopy to explore structure and activity relations of Pt/ZrO_2 catalysts for CO_2/CH_4 reforming. *Top. Catal.* **2000**, *10*, 295–305. [CrossRef]

21.　Zhang, Z.; Tsipouriari, V.; Efstathiou, A.; Verykios, X. Reforming of methane with carbon dioxide to synthesis gas over supported rhodium catalysts: I. Effects of support and metal crystallite size on reaction activity and deactivation characteristics. *J. Catal.* **1996**, *158*, 51–63. [CrossRef]

22.　Yang, S.; Maroto-Valiente, A.; Benito-Gonzalez, M.; Rodriguez-Ramos, I.; Guerrero-Ruiz, A. Methane combustion over supported palladium catalysts: I. Reactivity and active phase. *Appl. Catal. B: Environ.* **2000**, *28*, 223–233. [CrossRef]

23.　Moradi, G.R.; Rahmanzadeh, M.; Khosravian, F. The effects of partial substitution of Ni by Zn in $LaNiO_3$ perovskite catalyst for methane dry reforming. *J. CO_2 Util.* **2014**, *6*, 7–11. [CrossRef]

24.　Aparicio, L. Transient isotopic studies and microkinetic modeling of methane reforming over nickel catalysts. *J. Catal.* **1997**, *165*, 262–274. [CrossRef]

25.　García-Diéguez, M.; Pieta, I.; Herrera, M.; Larrubia, M.; Alemany, L. Nanostructured Pt-and Ni-based catalysts for CO_2-reforming of methane. *J. Catal.* **2010**, *270*, 136–145. [CrossRef]

26.　Mahoney, E.G.; Pusel, J.M.; Stagg-Williams, S.M.; Faraji, S. The effects of Pt addition to supported Ni catalysts on dry (CO_2) reforming of methane to syngas. *J. CO_2 Util.* **2014**, *6*, 40–44. [CrossRef]

27.　Vaidya, P.; Rodrigues, A.E. Insight into steam reforming of ethanol to produce hydrogen for fuel cells. *Chem. Eng. J.* **2006**, *117*, 39–49. [CrossRef]

28.　Haryanto, A.; Fernando, S.; Murali, N.; Adhikari, S. Current status of hydrogen production techniques by steam reforming of ethanol: A review. *Energy Fuels* **2005**, *19*, 2098–2106. [CrossRef]

29. de la Piscina, P.R.; Homs, N. Use of biofuels to produce hydrogen (reformation processes). *Chem. Soc. Rev.* **2008**, *37*, 2459–2467. [CrossRef] [PubMed]

30. Takanabe, K.; Aika, K.; Seshan, K.; Lefferts, L. Sustainable hydrogen from bio-oil—Steam reforming of acetic acid as a model oxygenate. *J. Catal.* **2004**, *227*, 101–108. [CrossRef]

31. Kumar, A.; Bhosale, R.R.; Malik, S.S.; Abusrafa, A.E.; Saleh, M.A.H.; Ghosh, U.K.; Al-Marri, M.J.; Almomani, F.A.; Khader, M.M.; Abu-Reesh, I.M. Thermodynamic investigation of hydrogen enrichment and carbon suppression using chemical additives in ethanol dry reforming. *Int. J. Hydrog. Energy* **2016**, *41*, 15149–15157. [CrossRef]

32. Ashraf, J.; Kumar, A. Thermodynamic evaluation of hydrazine assisted glycerol reforming for syngas production and coke inhibition. *Int. J. Hydrog. Energy* **2018**, *43*, 12999–13008. [CrossRef]

33. Kumar, A.; Mukasyan, A.S.; Wolf, E.E. Impregnated layer combustion synthesis method for preparation of multicomponent catalysts for the production of hydrogen from oxidative reforming of methanol. *Appl. catal. A General* **2010**, *372*, 175–183. [CrossRef]

34. Mukasyan, A.K.A.S.; Wolf, E.E. Modeling Impregnated Layer Combustion Synthesis of Catalyts for Hydrogen Generation from Oxidative Reforming of Methanol. *Ind. Eng. Chem. Res.* **2010**, *49*, 11001–11008.

35. Kumar, A.; Wolf, E.E.; Mukasyan, A.S. Solution combustion synthesis of metal nanopowders: Copper and copper/nickel alloys. *AIChE J.* **2011**, *57*, 3473–3479. [CrossRef]

36. Kumar, A.; Mukasyan, A.; Wolf, E. Combustion synthesis of Ni, Fe and Cu multi-component catalysts for hydrogen production from ethanol reforming. *Appl. Catal. A: General* **2011**, *401*, 20–28. [CrossRef]

37. Cross, A.; Kumar, A.; Wolf, E.E.; Mukasyan, A.S. Combustion Synthesis of a Nickel Supported Catalyst: Effect of Metal Distribution on the Activity during Ethanol Decomposition. *Ind. Eng. Chem. Res.* **2012**, *51*, 12004–12008. [CrossRef]

38. Kumar, A.; Miller, J.T.; Mukasyan, A.S.; Wolf, E.E. In situ XAS and FTIR studies of a multi-component Ni/Fe/Cu catalyst for hydrogen production from ethanol. *Appl. Catal. A: General* **2013**, *467*, 593–603. [CrossRef]

39. Ashok, A.; Kumar, A.; Bhosale, R.R.; Saleh, M.A.H.; van den Broeke, L.J. Cellulose assisted combustion synthesis of porous Cu–Ni nanopowders. *RSC Adv.* **2015**, *5*, 28703–28712. [CrossRef]

40. Kumar, A.; Cross, A.; Manukyan, K.; Bhosale, R.R.; van den Broeke, L.J.P.; Miller, J.T.; Mukasyan, A.S.; Wolf, E.E. Combustion synthesis of copper–nickel catalysts for hydrogen production from ethanol. *Chem. Eng. J.* **2015**, *278*, 46–54. [CrossRef]

41. Kumar, A.; Ashok, A.; Bhosale, R.R.; Saleh, M.A.H.; Almomani, F.A.; Al-Marri, M.; Khader, M.M.; Tarlochan, F. In situ DRIFTS Studies on Cu, Ni and CuNi catalysts for Ethanol Decomposition Reaction. *Catal. Lett.* **2016**, *146*, 778–787. [CrossRef]

42. Ashok, A.; Kumar, A.; Bhosale, R.R.; Saleh, M.A.H.; Ghosh, U.K.; Al-Marri, M.; Almomani, F.A.; Khader, M.M.; Tarlochan, F. Cobalt oxide nanopowder synthesis using cellulose assisted combustion technique. *Ceram. Int.* **2016**, *42*, 12771–12777. [CrossRef]

43. Ashok, A.; Kumar, A.; Bhosale, R.; Saad, M.A.S.; AlMomani, F.; Tarlochan, F. Study of ethanol dehydrogenation reaction mechanism for hydrogen production on combustion synthesized cobalt catalyst. *Int. J. Hydrog. Energy* **2017**, *42*, 23464–23473. [CrossRef]

44. Matin, M.; Kumar, A.; Bhosale, R.; Saad, M.S.; Almomani, F.; Al-Marri, M. PdZn nanoparticle electrocatalysts synthesized by solution combustion for methanol oxidation reaction in an alkaline medium. *RSC Adv.* **2017**, *7*, 42709–42717. [CrossRef]

45. Ashok, A.; Kumar, A.; Bhosale, R.R.; Almomani, F.; Malik, S.S.; Suslov, S.; Tarlochan, F. Combustion synthesis of bifunctional LaMO$_3$ (M=Cr, Mn, Fe, Co, Ni) perovskites for oxygen reduction and oxygen evolution reaction in alkaline media. *J. Electroanal. Chem.* **2018**, *809*, 22–30. [CrossRef]

46. Ashok, A.; Kumar, A.; Bhosale, R.; Almomani, F.; Saad, M.A.H.S.; Suslov, S.; Tarlochan, F. Influence of fuel ratio on the performance of combustion synthesized bifunctional cobalt oxide catalysts for fuel cell application. *Int. J. Hydrog. Energy* **2018**, in press. [CrossRef]

47. Matin, M.A.; Kumar, A.; Saad, M.A.H.S.; Al-Marri, M.J.; Suslov, S. Zn-enriched PtZn nanoparticle electrocatalysts synthesized by solution combustion for ethanol oxidation reaction in an alkaline medium. *MRS Commun.* **2018**, *8*, 411–419. [CrossRef]

48. Kumar, A.; Wolf, E.E.; Mukasyan, A.S. Solution Combustion Synthesis of Metal Nanopowders: Nickel-Reaction Pathways. *AIChE J.* **2011**, *57*, 2207–2214. [CrossRef]

49. Klerke, A.; Christensen, C.H.; Nørskov, J.K.; Vegge, T. Ammonia for hydrogen storage: Challenges and opportunities. *J. Mater. Chem.* **2008**, *18*, 2304–2310. [CrossRef]

50. Christensen, C.H.; Johannessen, T.; Sørensen, R.Z.; Nørskov, J.K. Towards an ammonia-mediated hydrogen economy? *Catal. Today* **2006**, *111*, 140–144. [CrossRef]

51. Jones, R. *Thermodynamics and Its Applications-an Overview*; Mintek: Randburg, South Afria, 1997.

52. Lide, D.R. *CRC Handbook of Chemistry and Physics: A Ready-Reference Book of Chemical and Physical Data*; CRC Press: Boca Raton, FL, USA, 2004.

53. Pakhare, D.; Shaw, C.; Haynes, D.; Shekhawat, D.; Spivey, J. Effect of reaction temperature on activity of Pt-and Ru-substituted lanthanum zirconate pyrochlores ($La_2Zr_2O_7$) for dry (CO_2) reforming of methane (DRM). *J. CO_2 Util.* **2013**, *1*, 37–42. [CrossRef]

54. Wang, W.; Herreros, J.M.; Tsolakis, A.; York, A.P. Ammonia as hydrogen carrier for transportation; investigation of the ammonia exhaust gas fuel reforming. *Int. J. Hydrogen Energy* **2013**, *38*, 9907–9917. [CrossRef]